Hindawi Publishing Corporation
EURASIP Journal on Wireless Communications and Networking
Volume 2010, Article ID 193183, 13 pages
doi:10.1155/2010/193183

Research Article

Probability of Error of Linearly Modulated Signals with Gaussian Cochannel Interference in Maximally Correlated Rayleigh Fading Channels

Luca Rugini and Paolo Banelli

Department of Electronic and Information Engineering, University of Perugia, Via G. Duranti 93, 06125 Perugia, Italy

Correspondence should be addressed to Luca Rugini, luca.rugini@diei.unipg.it

Received 30 November 2009; Revised 12 May 2010; Accepted 30 June 2010

Academic Editor: Guosen Yue

Copyright © 2010 L. Rugini and P. Banelli. This is an open access article distributed under the Creative Commons Attribution License, which permits unrestricted use, distribution, and reproduction in any medium, provided the original work is properly cited.

We evaluate the probability of error of linearly modulated signals, such as phase-shift keying (PSK) and quadrature amplitude modulation (QAM), in the presence of Gaussian cochannel interference (CCI) and Rayleigh fading channels. Specifically, we assume that the fading channel of the CCI is maximally correlated with the fading channel of the signal of interest (SOI). In practical applications, the maximal correlation of the CCI channel with the SOI channel occurs when the CCI is generated at the transmitter, such as the multiuser interference in downlink systems, or when a transparent repeater relays some thermal noise together with the SOI. We analytically evaluate the error probability by using a series expansion of generalized hypergeometric functions. A convenient truncation criterion is also discussed. The proposed theoretical approach favorably compares with alternative approaches, such as numerical integration and Monte Carlo estimation. Among the various applications of the proposed analysis, we illustrate the effect of nonlinear amplifiers in orthogonal frequency-division multiplexing (OFDM) systems, the downlink reception of code-division multiple-access (CDMA) signals, and the outdoor-to-indoor relaying of Global Positioning System (GPS) signals.

1. Introduction

Thermal noise, fading channels, and cochannel interference (CCI) are among the main sources of performance degradation in wireless communication systems. For fading channels, the theoretical evaluation of the system performance has been extensively explored in the technical literature (see [1, 2], and the references therein), mainly in terms of symbol-error probability, equivalently known as symbol-error rate (SER), and of bit-error probability, also called bit-error rate (BER). In the last decades, the BER analysis has been extended to include the presence of faded CCI. Krishnamurthi and Gupta have investigated the BER of QPSK and 8-PSK when the signal of interest (SOI) and a single interferer are affected by independent Rayleigh fading channels [3]. Beaulieu and Abu-Dayya have evaluated the BER of QPSK when the SOI is subject to Nakagami fading and the interferer is affected by Rayleigh fading [4]. The BER analysis in Nakagami fading channels has been subsequently extended by Aalo and Zhang to multiple interferers, whose CCI can be modeled as Gaussian, under the assumption that the SOI employs differential PSK [5]. The BER of BPSK-modulated SOI with multiple CCI subject to Rayleigh fading has been studied also in the presence of multiple receive antennas [6–8].

The common feature of all the mentioned research studies is that the fading experienced by the CCI is independent of the fading experienced by the SOI. However, in many practical scenarios, the fading channel of the CCI and the fading channel of the SOI are highly correlated [9, 10]. In some important cases, this correlation is at maximum level, for example, when both the SOI and the CCI are subject to the same fading channel. For instance, this scenario happens when the CCI is generated at the transmitter, such as the multiuser interference in code-division multiple-access (CDMA) downlink systems [11]. Other examples of transmitter-generated CCI include the nonlinear distortion caused by the high-power amplifier in orthogonal frequency-division multiplexing (OFDM) systems [12, 13], and the thermal noise produced by the front-end of a transparent transponder that relays Global Positioning System (GPS) signals from outdoor to an indoor receiver [14]. In all these scenarios, the CCI is well modeled by a Gaussian random variable. Despite the nonnegligible number of scenarios of interest, there have been few theoretical studies about the BER performance in the presence of CCI that is subject to the same fading channel of the SOI. Recently, Beaulieu and his coworkers have analyzed the BER performance when the SOI and the CCI experience correlated Rayleigh fading, assuming multiple receive antennas and maximal ratio combining [15, 16]. However, the analysis of [15, 16] is valid only for BPSK-modulated SOI, and for multiple interferers that use BPSK; therefore, the obtained results are not valid when the CCI is Gaussian.

In this paper, we develop a SER analysis for linear modulations in Rayleigh fading channels, when the CCI is modeled as Gaussian at the decision variable. The proposed analysis can be employed in order to predict the maximum amount of interference that can be tolerated at the receiver, given a fixed performance requirement. We focus on maximally correlated fading channels, that is, we assume that the CCI is subject to the same fading channel that affects the SOI. Specifically, we analytically assess the error probability by using a series expansion of *generalized hypergeometric functions* [17]. Different aspects of the proposed formula are considered, such as, alternative expressions, series truncation criterion, BER with Gray coding, and effect of phase errors. We compare the proposed analysis with two alternative approaches, that is, numerical and statistical. The numerical approach uses *Laguerre-Gauss quadrature* [18] to evaluate the SER expressed as a single integral of a real variable. The statistical approach estimates the SER by means of a Monte Carlo method that shares many similarities with *semianalytic evaluation* [19]. We show that the proposed theoretical method enjoys a better accuracy with respect to both numerical and statistical methods, and that our theoretical results can accurately predict the SER performance in many different scenarios. Specifically, we focus on three applications: OFDM systems subject to high-power amplifier nonlinearities, CDMA detectors impaired by multiuser interference in downlink transmissions, and GPS receivers aided by outdoor-to-indoor relays. However, our analysis is quite general, since it can be applied to any communication system that is impaired by Gaussian CCI generated at the transmitter, when the channel experiences Rayleigh fading. Note that for some particular cases, the CCI generated at the receiver can be interpreted as generated at the transmitter. This happens, for instance, in OFDM systems affected by carrier frequency offset, where the frequency mismatch between the local oscillators of the receiver and of the transmitter can be attributed to the transmitter [20]. Our analysis is valid for these particular cases as well.

The remainder of this paper is organized as follows. In Section 2, we analytically evaluate the error probability and discuss how to safely truncate the resulting series expansion. Section 3 compares the proposed analysis with alternative approaches based on numerical integration or on Monte Carlo methods. In Section 4, we show that our theoretical results closely characterize the error performance in different application scenarios. Section 5 contains some concluding remarks.

2. Error Probability Analysis

We consider a signal model expressed by

$$\tilde{z}[m] = c[m]s[m] + c[m]i[m] + \tilde{n}[m], \tag{1}$$

where $\tilde{z}[m]$ is the signal received at the time index m, $c[m]$ is the complex-valued coefficient that represents the slow flat-fading channel, $s[m]$ is the SOI, characterized by zero mean and power σ_{S}^2, $i[m]$ is the circularly-symmetric complex Gaussian CCI, with zero mean and power σ_{I}^2, and $\tilde{n}[m]$ is the zero-mean additive white Gaussian noise (AWGN) at the receiver side, with power σ_{N}^2. The symbols $s[m]$, independent and identically distributed, are drawn from a common constellation like QAM or PSK. The three signals $s[m]$, $i[m]$, and $\tilde{n}[m]$, as well as the channel coefficient $c[m]$, are assumed as mutually independent. From (1), it is obvious that the two fading channels experienced by the SOI and by the CCI are maximally correlated, because the coefficient $c[m]$ is the same for both SOI and CCI.

Since we assume symbol-rate sampling and symbol-by-symbol detection, we drop the time index m. Rayleigh fading is assumed, that is, by expressing the channel coefficient as $c = re^{j\theta}$, the probability density function (pdf) of the envelope r is expressed by [2]

$$p(r) = \frac{2r}{\Omega} e^{-r^2/\Omega} \mathrm{u}(r), \tag{2}$$

where $\mathrm{u}(r)$ is the unit step function and $\Omega = E\{r^2\}$. The phase θ, independent of r, is uniformly distributed in $[0, 2\pi)$. We first assume that the receiver is able to perfectly compensate for the phase shift θ introduced by the channel. Therefore, the decision variable is $z = e^{-j\theta}\tilde{z}$, which is expressed by

$$z = rs + ri + n, \tag{3}$$

where $n = e^{-j\theta}\tilde{n}$.

In order to analytically evaluate the SER in fading channels, different methods are available, such as the direct method (also known as the pdf method), the moment generating function (MGF) method, and the characteristic function (CHF) method [2, 21]. Basically, the symbol-error probability P_e is obtained by averaging the conditional symbol-error probability $P_{ec}(r)$ over the fading statistics $p(r)$, as expressed by

$$P_e = \int_0^{+\infty} P_{ec}(r) p(r) dr. \tag{4}$$

The direct method consists in analytically solving the integral in (4), after that the pdf $p(r)$ has been calculated. On the contrary, the MGF (or the CHF) method translates the problem (4) into the frequency domain, by exploiting the Laplace (or the Fourier) transform of $p(r)$ [2, 21]. Usually, the MGF and the CHF methods are convenient when $p(r)$ is difficult to obtain [21]. In our case, $p(r)$ is known and therefore we employ the direct method.

When conditioned on the fading envelope r, the overall interference-plus-noise term $ri + n$ in (3) is Gaussian distributed. Therefore, the conditional symbol-error probability $P_{ec}(r)$ can be expressed by

$$P_{ec}(r) = \alpha Q\left(\sqrt{\gamma\rho(r)}\right), \tag{5}$$

where $Q(x) = (2\pi)^{-1/2}\int_x^{+\infty} e^{-\nu^2/2}d\nu$ is the Q-function [22], $\rho(r)$ is the conditional signal-to-interference-plus-noise ratio (SINR), expressed by

$$\rho(r) = \frac{r^2\sigma_{\mathrm{S}}^2}{r^2\sigma_{\mathrm{I}}^2 + \sigma_{\mathrm{N}}^2}, \tag{6}$$

and α and γ are two constants that depend on the constellation format. Actually, (5) is exact only for BPSK [23], but it is a good approximation for both M-PSK with constellation size $M > 2$ and M-QAM [2]. Although (5), for M-PSK and M-QAM, could be replaced by

$$P_{ec}(r) = \sum_{i=1}^{N_{\mathrm{Q}}}\alpha_i Q\left(\sqrt{\gamma_i\rho(r)}\right), \tag{7}$$

where N_{Q} is an appropriate number of terms, here we use (5) for simplicity. By inserting (5), (6), and (2) in (4), the symbol-error probability P_e becomes

$$P_e = 2\alpha\int_0^{+\infty} Q\left(\sqrt{\gamma\frac{r^2\sigma_{\mathrm{S}}^2}{r^2\sigma_{\mathrm{I}}^2 + \sigma_{\mathrm{N}}^2}}\right)\frac{r}{\Omega}e^{-r^2/\Omega}dr. \tag{8}$$

The integrals 1of the same kind of (8), in the past, have been considered complicated to solve [11], mainly because the conditional symbol-error probability $P_{ec}(r)$ is a complicated function of r. However, an analytical solution of (8) exists, and its derivation is shown in Appendix A. The solution of (8) can be expressed as

$$\begin{aligned} P_e = {} & \frac{\alpha}{2} - \frac{\alpha\sqrt{2\gamma\Omega}}{4}\frac{\sigma_{\mathrm{S}}}{\sigma_{\mathrm{N}}}e^{-(\gamma/2)\sigma_{\mathrm{S}}^2/\sigma_{\mathrm{I}}^2}\sum_{k=0}^{+\infty}\frac{1}{k!}\left(\frac{\gamma}{2}\frac{\sigma_{\mathrm{S}}^2}{\sigma_{\mathrm{I}}^2}\right)^k \\ & \times {}_2F_0\left(k+\frac{3}{2},\frac{1}{2};;-\Omega\frac{\sigma_{\mathrm{I}}^2}{\sigma_{\mathrm{N}}^2}\right), \end{aligned} \tag{9}$$

where ${}_pF_q(\cdot)$ stands for the generalized hypergeometric function [17], defined by

$${}_pF_q\left(a_1,\ldots,a_p;b_1,\ldots,b_q;x\right) = \sum_{l=0}^{+\infty}\frac{(a_1)_l\ldots\left(a_p\right)_l}{(b_1)_l\ldots\left(b_q\right)_l}\frac{x^l}{l!}, \tag{10}$$

where $(a)_l = \Gamma(a+l)/\Gamma(a)$ is the Pochhammer's symbol (or rising factorial) expressed in terms of the Gamma function [22]. Instead of (9), the symbol-error probability P_e can be equivalently expressed using alternative formulas, as detailed in Appendix B. We highlight that the solution (9) of (8) is exact, that is, it does not involve any approximation of the Q-function [24, 25].

2.1. Truncation Criterion. For practical purposes, the evaluation of (9) requires a truncation of the infinite series. As a consequence, we investigate how many terms (and which ones) are necessary to obtain an accurate approximation of the exact result. To evaluate the effect of the truncation error, we resort to a mixed approach that uses both graphical considerations and analytical approximations. Specifically, we express (9) as

$$P_e = \alpha\left(\frac{1}{2} - \sum_{k=0}^{+\infty}t(k)\right), \tag{11}$$

$$t(k) = \frac{\sqrt{2\rho_{\mathrm{N}}}}{4}e^{-\rho_{\mathrm{I}}/2}\frac{1}{k!}\left(\frac{\rho_{\mathrm{I}}}{2}\right)^k {}_2F_0\left(k+\frac{3}{2},\frac{1}{2};;-\frac{\rho_{\mathrm{N}}}{\rho_{\mathrm{I}}}\right), \tag{12}$$

where the parameters $\rho_{\mathrm{I}} = \gamma\sigma_{\mathrm{S}}^2/\sigma_{\mathrm{I}}^2$ and $\rho_{\mathrm{N}} = \gamma\Omega\sigma_{\mathrm{S}}^2/\sigma_{\mathrm{N}}^2$ represent the scaled signal-to-interference ratio (SIR) and the scaled signal-to-noise ratio (SNR), respectively. The scaling factor γ, which is the same for both ratios, accounts for different constellations. Figures 1, 2, and 3 show that the shape of $t(k)$ in (12) is almost independent of the scaled SNR ρ_{N}, and it practically depends on the scaled SIR ρ_{I} only. In particular, Figure 3 can be used to select only the relevant terms of the series in (9). Interestingly, these relevant terms are adjacent, and therefore a very good approximation of the exact SER in (9) can be obtained as

$$P_{e,\mathrm{approx}} = \alpha\left(\frac{1}{2} - \sum_{k=k_{\min}}^{k_{\max}}t(k)\right), \tag{13}$$

by a convenient choice of $k_{\min}$ and $k_{\max}$. By using (13) instead of (11), the computational complexity of the SER evaluation is reduced, especially when the number of terms $\kappa = k_{\max} - k_{\min} + 1$ is low. Note that since the term $t(k)$ is nonnegative, $P_{e,\mathrm{approx}} \geq P_e$, that is, the approximation (13) is an upper bound.

To determine $k_{\min}$ and $k_{\max}$, we exploit the two following observations, suggested by Figure 3:

(i) $t(k)$ has a parabolic-like shape in the logarithmic scale, and hence a Gaussian-like shape in the linear scale.

(ii) For sufficiently high values of the scaled SIR ρ_{I}, the maximum of $t(k)$ is obtained when $k \approx \lfloor\rho_{\mathrm{I}}/2\rfloor$.

Hence, in order to find $k_{\min}$ and $k_{\max}$, we approximate $t(k)$ with the Gaussian function $G(k)$ expressed by

$$G(k) = \frac{A}{\sqrt{2\pi}\sigma}e^{-(k-\eta)^2/(2\sigma^2)}, \tag{14}$$

where the mean value is $\eta = \lfloor\rho_{\mathrm{I}}/2\rfloor$, and A and σ are two parameters to be determined. We have

$$A = \int_{-\infty}^{+\infty}G(x)dx \approx \int_0^{+\infty}G(x)dx \approx \sum_{k=0}^{+\infty}t(k) = \frac{1}{2} - \frac{P_e}{\alpha} \approx \frac{1}{2}, \tag{15}$$

where the first approximation is valid when the scaled SIR ρ_{I}, or equivalently η, is sufficiently high, while the last

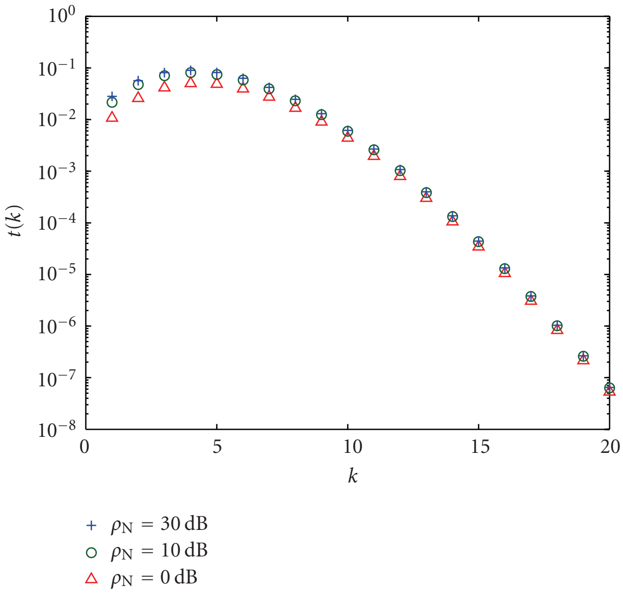

FIGURE 1: Evaluation of $t(k)$ in (12) when ρ_I = 10 dB.

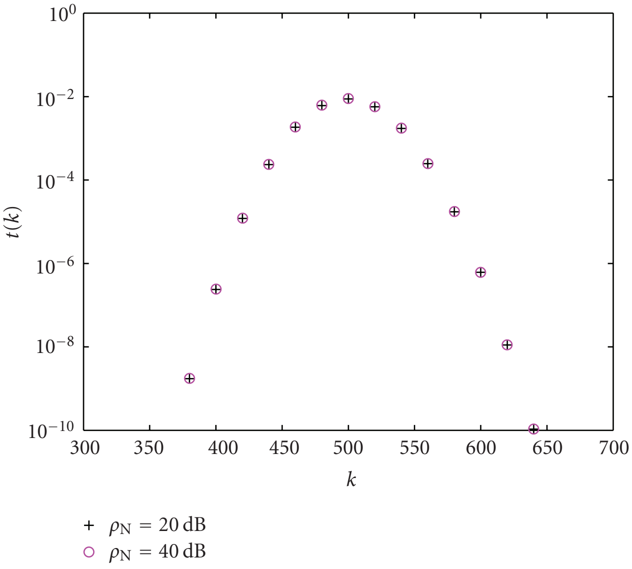

FIGURE 2: Evaluation of $t(k)$ in (12) when ρ_I = 30 dB.

approximation is valid when the symbol-error probability P_e is sufficiently low. Therefore, we set $A = 1/2$. In order to determine σ, we impose $G(\eta) = t(\eta)$, which leads to

$$\sigma = \frac{1}{2\sqrt{2\pi}t(\lfloor \rho_I/2 \rfloor)}. \tag{16}$$

As a result, our truncation criterion selects $k_{\min} = \max\{\lfloor \eta - T\sigma \rfloor, 0\}$, and $k_{\max} = \lceil \eta + T\sigma \rceil$, where T is a parameter that controls the approximation accuracy of (13). This parameter can be chosen by exploiting the Gaussian integral properties and by denoting with ε the approximation error introduced by (13), we have

TABLE 1: Parameters of the series truncation for $T = 6$ and $\rho_N = 1000$.

ρ_I (dB)	η	σ	$k_{\min}$	$k_{\max}$	κ
10	5	2.442	0	20	21
15	15	3.975	0	39	40
20	50	7.143	7	93	87
25	158	12.61	82	234	153
30	500	22.40	365	635	271
35	1581	39.81	1342	1820	479
40	5000	70.79	4575	5425	851
45	15811	125.9	15055	16567	1513
50	50000	223.8	48657	51343	2687

$$\begin{aligned}\varepsilon &= \alpha \sum_{k=0}^{k_{\min}-1} t(k) + \alpha \sum_{k=k_{\max}+1}^{+\infty} t(k) \\ &\approx \alpha \int_{-\infty}^{\eta - T\sigma} G(x)dx + \alpha \int_{\eta+T\sigma}^{+\infty} G(x)dx = \alpha Q(T).\end{aligned} \tag{17}$$

Therefore, assuming a maximum error ε, T can be chosen as $T = Q^{-1}(\varepsilon/\alpha)$. For instance, in QPSK, where $\alpha = 1$, an approximation error $\varepsilon \approx 10^{-3}$ is expected when $T = 3$, while $\varepsilon \approx 10^{-9}$ for $T = 6$. The proposed criterion also permits to check whether the approximated SER in (13) is acceptable within a desired accuracy (e.g., relative error lower than or equal to 1%), by simply checking whether $\alpha Q(T) \leq 10^{-2}(P_{e,\text{approx}} + \alpha Q(T))$ is verified or not. If it is not verified, the value of T should be increased further.

Figure 4 confirms that the proposed truncation criterion produces accurate results. Indeed, when $T = 3$, the approximation error is $\varepsilon \approx 10^{-3}$, as expected. Table 1 shows the values of $k_{\min}$ and $k_{\max}$, as well as the number of terms κ, for $T = 6$ when ρ_N = 30 dB. From Table 1, it is clear that for low values of the scaled SIR ρ_I, the number of terms κ is relatively small. On the other hand, for higher values of ρ_I, κ increases considerably. However, in this case, the variability of $t(k)$ with respect to k is reduced, that is, $t(k+1) \approx t(k)$. Consequently, the κ terms are not all necessary, and only a single term out of F consecutive terms can be evaluated. This way, the evaluation complexity is reduced by a factor F, by exploiting

$$\sum_{k=k_{\min}}^{k_{\max}} t(k) \approx F \sum_{\substack{k=k_{\min} \\ k \bmod F=0}}^{k_{\max}} t(k). \tag{18}$$

2.2. Bit-Error Probability. In many cases, the bit-error probability, or BER, is a preferred performance indicator with respect to the symbol-error probability. Anyway, the presented SER approach can be easily extended to the BER evaluation. Indeed, for M-QAM and M-PSK with Gray coding, assuming that M is a power of two, the BER can be expressed as a linear combination of Q-functions with

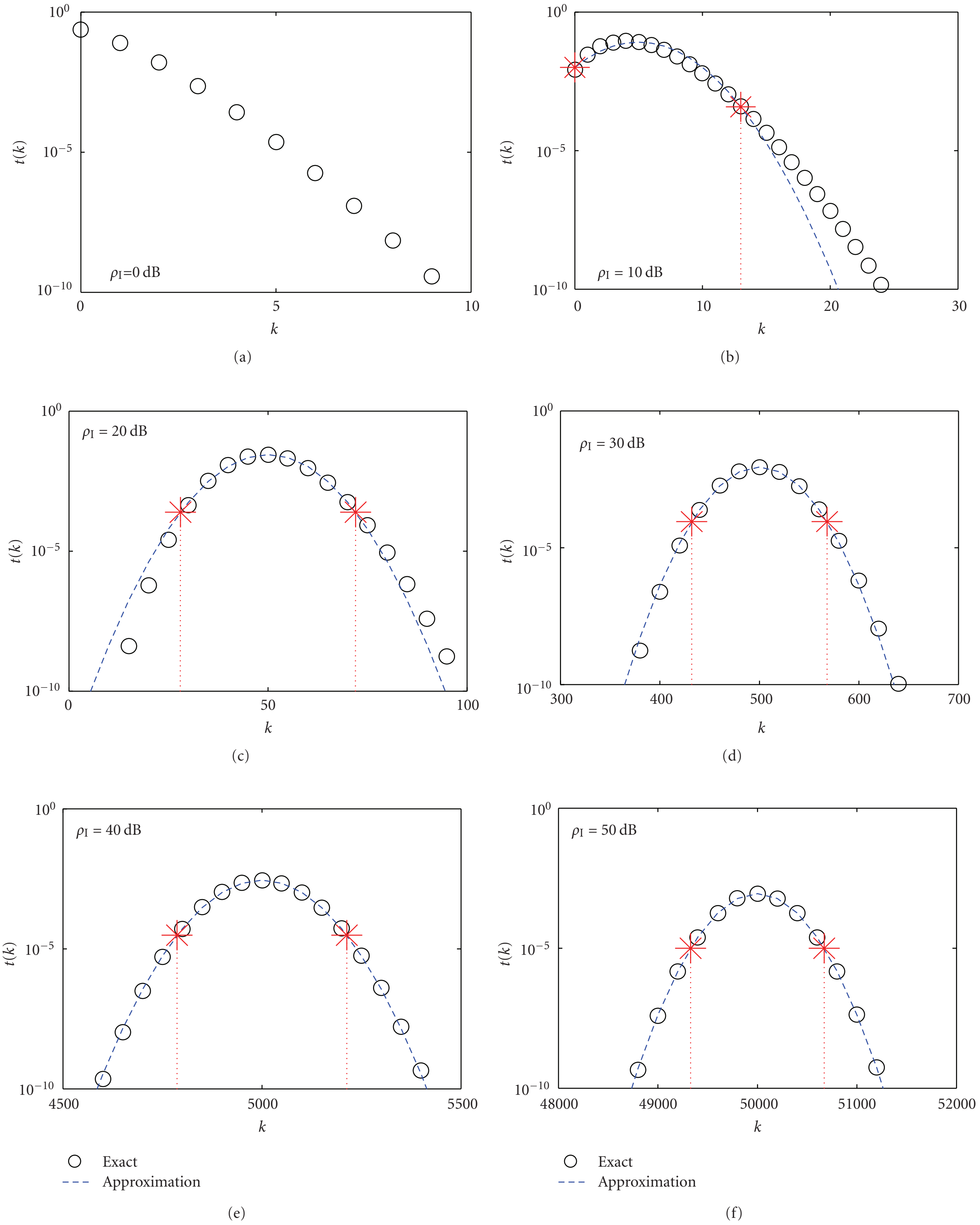

FIGURE 3: Evaluation of $t(k)$ when $\rho_N = 30$ dB. Comparison between the exact value in (12) and the approximation in (14). The asterisks denote $k_{\min}$ and $k_{\max}$ obtained for $T = 3$.

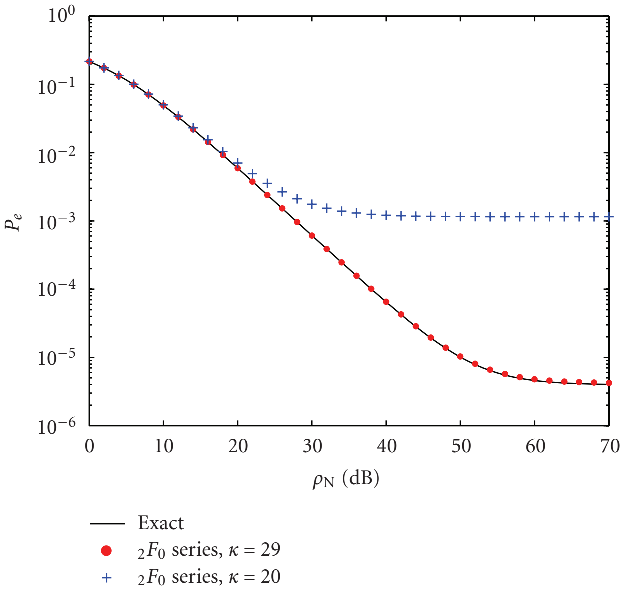

Figure 4: Effect of the truncation error ($\rho_I = 13$ dB). For $T = 3$ ($T = 6$), our criterion produces $\kappa = 20$ ($\kappa = 29$). The exact curve is obtained by using $\kappa = 101$. In all three cases, $k_{\min} = 0$.

different arguments [26, 27], similarly to the SER in (7). For instance, the exact conditional BER for square M-QAM with Gray coding is expressed by [26]

$$P_{cbe}^{M\text{-QAM}}(r) = \frac{1}{\sqrt{M}\log_2\sqrt{M}} \sum_{j=1}^{\log_2\sqrt{M}} \sum_{i=0}^{(1-2^{-j})\sqrt{M}-1} (-1)^{\lfloor 2^{j-1} i/\sqrt{M}\rfloor} \times \left(2^j - 2\left\lfloor \frac{2^{j-1} i}{\sqrt{M}} + \frac{1}{2}\right\rfloor\right) Q\left(\sqrt{\frac{3(2i+1)^2}{M-1}\rho(r)}\right) \quad (19)$$

while a very good approximation for M-PSK with Gray coding is expressed by [27]

$$P_{cbe}^{M\text{-PSK}}(r) \approx \frac{2}{\max\{\log_2 M, 2\}} \sum_{i=1}^{\max\{M/4,1\}} Q\left(\sqrt{2\rho(r)\sin^2\frac{(2i-1)\pi}{M}}\right), \quad (20)$$

where $\rho(r)$ is the SINR per symbol, expressed by (6). In both cases, the conditional BER is expressed as a finite sum of weighted Q-functions. Therefore, the final BER averaged over the fading channel will be a finite sum of terms, each one expressed by (9), with a convenient definition of the parameters α and γ. There are also other constellations whose conditional BER can be expressed as a finite sum of weighted Q-functions, such as rectangular QAM [26], cross QAM [28], and hierarchical QAM [29]. Our approach is valid for these constellations too.

2.3. Effect of Phase Error. We have assumed so far that the phase shift θ introduced by the channel has been perfectly estimated and compensated. We now remove this limitation and assume that the received sample is obtained as $\hat{z} = e^{-j\hat{\theta}}\tilde{z}$, where $\hat{\theta}$ is an estimate of θ. Therefore, we have

$$\hat{z} = re^{j\theta_e}s + re^{j\theta_e}i + e^{j\theta_e}n, \quad (21)$$

where $\theta_e = \theta - \hat{\theta}$ is the phase error. Since the CCI i is circularly Gaussian, $\hat{i} = e^{j\theta_e}i$ in (21) has the same statistical properties of i. The same property holds true also for the AWGN term n. As a result, the phase error θ_e only affects the SOI. If we assume that θ_e is deterministic (non random), the additional multiplicative term $e^{j\theta_e}$ mixes the I/Q components and practically acts as an SINR loss that increases the conditional symbol-error probability $P_{ec}(r)$. For BPSK and QPSK, when $\theta_e \neq 0$, (5) is replaced by the following expression

$$\begin{aligned} P_{ec}^{\text{BPSK}}(r) &= \alpha Q\left(\sqrt{\gamma\cos^2\theta_e\rho(r)}\right), \\ P_{ec}^{\text{QPSK}}(r) &= \frac{\alpha}{2} Q\left(\sqrt{\gamma(1-\sin 2\theta_e)\rho(r)}\right) \\ &\quad + \frac{\alpha}{2} Q\left(\sqrt{\gamma(1+\sin 2\theta_e)\rho(r)}\right), \end{aligned} \quad (22)$$

respectively, where $\alpha = 1$ and $\gamma = 2$ for BPSK, and $\alpha = \gamma = 1$ for QPSK. Therefore, the proposed analysis can be applied also in the presence of phase errors, by incorporating the factors $\cos^2\theta_e$, $1 - \sin 2\theta_e$, and $1 + \sin 2\theta_e$, into the parameter γ in (9).

2.4. Lower Bounds. The truncation criterion described in Section 2.1 can be interpreted as a tight upper bound on the SER. Here, we derive some simple lower bounds obtained by neglecting the AWGN with respect to the CCI, and vice versa. When the AWGN power σ_N^2 is equal to zero, from (8) it follows

$$P_e \geq P_{e,\text{LB1}} = 2\alpha \int_0^{+\infty} Q\left(\sqrt{\gamma\frac{\sigma_S^2}{\sigma_I^2}}\right)\frac{r}{\Omega}e^{-r^2/\Omega}dr = \alpha Q\left(\sqrt{\rho_I}\right), \quad (23)$$

which of course depends only on the scaled SIR $\rho_I = \gamma\sigma_S^2/\sigma_I^2$. Clearly, the lower bound (LB) (23) is valid independently of the channel pdf, provided that the CCI is Gaussian. Conversely, when the CCI power σ_I^2 is equal to zero, from (8) we obtain

$$\begin{aligned} P_e \geq P_{e,\text{LB2}} &= 2\alpha \int_0^{+\infty} Q\left(\sqrt{\gamma\frac{r^2\sigma_S^2}{\sigma_N^2}}\right)\frac{r}{\Omega}e^{-r^2/\Omega}dr \\ &= \frac{\alpha}{2}\left(1 - \sqrt{\frac{\rho_N}{2+\rho_N}}\right), \end{aligned} \quad (24)$$

which obviously depends only on the scaled SNR $\rho_N = \gamma\Omega\sigma_S^2/\sigma_N^2$. The LB (24) represents the classical error performance in (CCI-free) Rayleigh fading scenarios [23]. Section 4 will confirm that (9) fulfills both the lower bounds (23) and (24).

2.5. Extension to Signal-Dependent Interference or to Partially Correlated Channels.

In the system model expressed by (1) and (3), we have made two main assumptions.

(A1) The CCI i is independent of the SOI s.

(A2) The CCI and the SOI experience the same fading channel $c = re^{j\theta}$, that is, the channel coefficients of the CCI and of the SOI are maximally correlated.

In this subsection, we show that the results obtained in the previous subsections can be used also when one of the two assumptions is no longer valid. First, let us assume that Assumption (A1) is not valid; that is, the CCI and the SOI are correlated (and consequently dependent), while maintaining Assumption (A2). Specifically, we replace Assumption (A1) with

(B1) $i = a_\mathrm{I} s + i_\mathrm{IND}$, where $a_\mathrm{I} = E\{is^*\}/E\{|s|^2\}$ is a constant, characterized by $|a_\mathrm{I}| < 1$, that takes into account the crosscorrelation between the CCI and the SOI, and i_IND is a zero-mean circularly symmetric complex Gaussian random variable independent of s.

Using Assumption (B1), the CCI i is a SOI-dependent Gaussian mixture. In this case, (1) becomes

$$\tilde{z} = cs + c(a_\mathrm{I} s + i_\mathrm{IND}) + \tilde{n} = c(1 + a_\mathrm{I})s + ci_\mathrm{IND} + \tilde{n}, \tag{25}$$

which is clearly in the same form of (1): now the SOI includes the multiplicative coefficient $1 + a_\mathrm{I}$, while the CCI i_IND is independent of the SOI. Therefore, when a_I is known, the error probability can be analyzed using the same approach described in the previous subsections, by including the coefficient $|1 + a_\mathrm{I}|^2$ into the SOI power.

Next, let us maintain Assumption (A1), and assume that (A2) is not valid, that is, the channel coefficients c_I of the CCI and c_S of the SOI are different, though both zero-mean Gaussian distributed. Specifically, we replace Assumption (A2) with

(B2) $c_\mathrm{I} = a_\mathrm{C} c_\mathrm{S} + c_\mathrm{IND}$, where $a_\mathrm{C} = E\{c_\mathrm{I} c_\mathrm{S}^*\}/E\{|c_\mathrm{S}|^2\}$ is a constant, characterized by $|a_\mathrm{C}| < 1$, that takes into account the crosscorrelation between the fading channels of the CCI and of the SOI, and c_IND is a zero-mean circularly symmetric complex Gaussian random variable independent of c_S.

Using Assumption (B2), the two fading channels c_I and c_S are partially correlated. In this case, (1) becomes

$$\begin{aligned} \tilde{z} &= c_\mathrm{S} s + c_\mathrm{I} i + \tilde{n} = c_\mathrm{S} s + (a_\mathrm{C} c_\mathrm{S} + c_\mathrm{IND}) i + \tilde{n} \\ &= c_\mathrm{S} s + c_\mathrm{S} a_\mathrm{C} i + \tilde{n}_\mathrm{TOT}, \end{aligned} \tag{26}$$

where $\tilde{n}_\mathrm{TOT} = c_\mathrm{IND} i + \tilde{n}$. Since the product of two zero-mean independent Gaussian random variables is characterized by a K_0-Bessel pdf (see [30, Equation 6.2]), the pdf of each component (real or imaginary) of $\tilde{n}_\mathrm{TOT} = c_\mathrm{IND} i + \tilde{n}$ is the convolution between a K_0-Bessel function and a Gaussian function. Therefore, $\tilde{n}_\mathrm{TOT}$ is in general non-Gaussian. However, when $c_\mathrm{IND} i$ and $\tilde{n}$ have approximately the same power, or when the thermal noise $\tilde{n}$ dominates, a Gaussian approximation for $\tilde{n}_\mathrm{TOT}$ is reasonable, and hence the previous analysis can be employed as well.

When both Assumptions (A1) and (A2) are replaced by (B1) and (B2), (1) becomes

$$\begin{aligned} \tilde{z} &= c_\mathrm{S} s + c_\mathrm{I} i + \tilde{n} = c_\mathrm{S} s + (a_\mathrm{C} c_\mathrm{S} + c_\mathrm{IND})(a_\mathrm{I} s + i_\mathrm{IND}) + \tilde{n} \\ &= c_\mathrm{S}(1 + a_\mathrm{C} a_\mathrm{I}) s + c_\mathrm{S} a_\mathrm{C} i_\mathrm{IND} + \tilde{n}_\mathrm{TOT}, \end{aligned} \tag{27}$$

where $\tilde{n}_\mathrm{TOT} = c_\mathrm{IND} a_\mathrm{I} s + c_\mathrm{IND} i_\mathrm{IND} + \tilde{n}$. Now $\tilde{n}_\mathrm{TOT}$ includes the SOI-dependent term $c_\mathrm{IND} a_\mathrm{I} s$, which is a Gaussian mixture, and hence an analysis based on the Gaussian approximation of $\tilde{n}_\mathrm{TOT}$ could lead to deceiving results.

3. Numerical Methods

In Section 2, we have presented an analytical method to evaluate the symbol-error probability. Alternatively, since the symbol-error probability (8) is expressed as a unique definite integral, numerical integration methods could be used. In this section, we present the SER results obtained using a numerical integration method known as *Laguerre-Gauss quadrature* [18]. In addition, we consider a statistical approach that makes use of *Monte Carlo integration*.

3.1. Laguerre-Gauss Quadrature.

Laguerre-Gauss (LG) quadrature, also known as Gauss-Laguerre quadrature, is a Gauss quadrature over the interval $[0, +\infty)$ with weighting function $W(x) = e^{-x}$ [18, 22]. By using the change of variables $x = r^2/\Omega$, (8) becomes

$$P_e = \alpha \int_0^{+\infty} Q\left(\sqrt{\gamma \frac{x\Omega\sigma_\mathrm{S}^2}{x\Omega\sigma_\mathrm{I}^2 + \sigma_\mathrm{N}^2}}\right) e^{-x} dx, \tag{28}$$

which is suitable for LG quadrature. Indeed, LG quadrature performs the approximation

$$\int_0^{+\infty} e^{-x} f(x) dx \approx \sum_{k=1}^{\kappa} w_k f(x_k), \tag{29}$$

where κ is the number of terms, x_k is the kth zeros of the Laguerre polynomial $L_\kappa(x)$, and

$$w_k = \frac{x_k}{(\kappa + 1)^2 [L_{\kappa+1}(x_k)]^2}, \tag{30}$$

is the kth weight [18, 22]. Consequently, we have

$$P_e \approx P_e^\mathrm{LG} = \alpha \sum_{k=1}^{\kappa} \frac{x_k}{(\kappa + 1)^2 [L_{\kappa+1}(x_k)]^2} Q\left(\sqrt{\gamma \frac{x_k\Omega\sigma_\mathrm{S}^2}{x_k\Omega\sigma_\mathrm{I}^2 + \sigma_\mathrm{N}^2}}\right). \tag{31}$$

The main difficulty of (31) arises when the number of terms κ increases, since the computational complexity also increases. Note that for a fixed κ, the abscissas x_k and the weights w_k are constant, and hence can be stored.

Figure 5 illustrates the symbol-error probability obtained with LG quadrature, in the same scenario of Figure 4. Clearly, the approximation error is relevant, even when $\kappa = 512$ terms are used in (31). However, as shown in Figure 4, our analytical approach, summarized by (12)-(13), produces accurate results by summing $\kappa = 29$ terms only.

3.2. Monte Carlo Integration. Monte Carlo (MC) integration is a statistical approach that evaluates the symbol-error probability by means of repeated outcomes of a computer-generated random variable. The core idea is the following approximation:

$$P_e = \int_0^{+\infty} P_{ec}(r)p(r)dr \approx \frac{1}{\kappa}\sum_{k=1}^{\kappa} P_{ec}(r_k), \qquad (32)$$

where $\{r_k\}_{k=1}^{\kappa}$ are i.i.d. randomly generated numbers with pdf $p(r)$, and κ is the number of outcomes. Specifically, the integral (8) is approximated as

$$P_e \approx P_e^{\mathrm{MC}} = \frac{\alpha}{\kappa}\sum_{k=1}^{\kappa} Q\left(\sqrt{\gamma\frac{r_k^2\sigma_{\mathrm{S}}^2}{r_k^2\sigma_{\mathrm{I}}^2+\sigma_{\mathrm{N}}^2}}\right), \qquad (33)$$

where r_k is Rayleigh distributed with the same pdf of r in (2). Noteworthy, this MC method can be interpreted as a *semianalytic* way to evaluate the symbol-error probability [19]. Indeed, in (33), the stochastic variability due to the constellation symbols and to the noise is analytically treated by using the Q-function, whereas the stochastic variability caused by the fading channel is simulated by means of repeated trials. This leads to a mixed analytical-simulated approach. Differently, pure simulation approaches employ repeated trials to generate not only the channel realizations, but also the symbol realizations and the noise realizations. The key feature of MC methods is that they can be used for any pdf $p(r)$. However, for specific distributions, such as Rayleigh, the analytical approach could be more accurate.

Figure 6 displays the symbol-error probability obtained with MC integration, in the same scenario of Figures 4 and 5. It is evident that using $\kappa = 2^{16} = 65536$ does not guarantee a good approximation, in contrast with the $\kappa = 29$ terms used by the analytical approach.

4. Applications

Herein we apply our theoretical method to evaluate the SER performance in three practical scenarios: OFDM systems subject to high-power amplifier nonlinearities, downlink CDMA systems in the presence of multiuser interference, and GPS receivers equipped with outdoor-to-indoor relays. However, there exist many other scenarios of interest, not considered in this paper for sake of conciseness. For instance, the proposed analytical approach can be used to predict the error performance of OFDM systems in the presence of intercarrier interference caused by carrier frequency offsets [20], of decorrelating multiuser receivers in nonlinear channels [31], and of multicarrier CDMA systems with transmitter-generated impairments [32]. In all these cases, maximal correlation between the fading channel of the SOI and of the CCI is experienced.

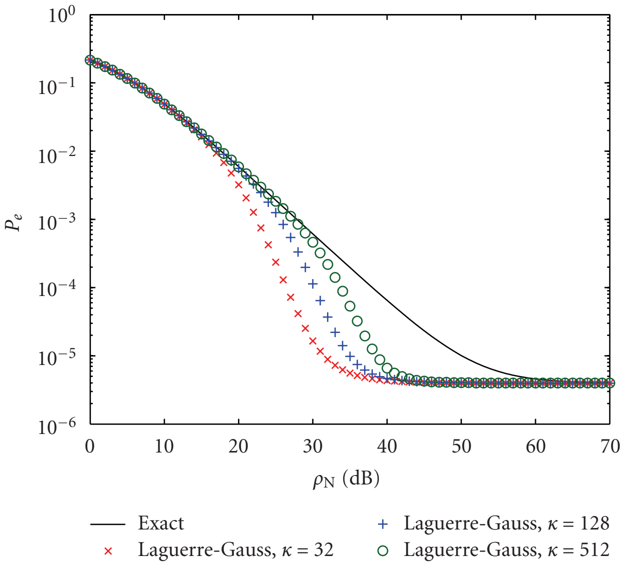

FIGURE 5: Approximation by Laguerre-Gauss quadrature ($\rho_{\mathrm{I}} = 13$ dB).

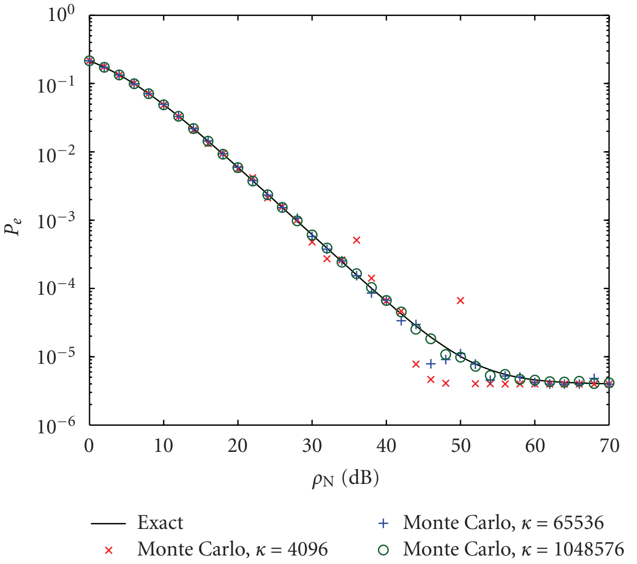

FIGURE 6: Approximation by Monte Carlo integration ($\rho_{\mathrm{I}} = 13$ dB).

4.1. OFDM with Nonlinear Amplification and Frequency-Selective Fading. The generic block of an OFDM system with K subcarriers can be expressed as $\mathbf{u} = \mathbf{T}_{\mathrm{CP}}\mathbf{F}^H\mathbf{s}$ [33], where $\mathbf{s}$ is the column vector of data symbols, $\mathbf{F}$ is the $K \times K$ unitary FFT matrix, and $\mathbf{T}_{\mathrm{CP}}$ is the $(K+L)\times K$ matrix that inserts the cyclic prefix (CP) of length L. After high-power amplification by means of an instantaneous nonlinear amplifier (NLA), by exploiting the Bussgang theorem, and assuming that the number of subcarriers is sufficiently high (e.g., $K > 32$), the transmitted block can be modeled by [12, 13]

$$\mathbf{v} = \tilde{\alpha}\mathbf{u} + \mathbf{d} = \tilde{\alpha}\mathbf{T}_{\mathrm{CP}}\mathbf{F}^H\mathbf{s} + \mathbf{T}_{\mathrm{CP}}\mathbf{i}_{\mathrm{NL}}, \qquad (34)$$

where $\tilde{\alpha}$ represents the average linear amplification gain, and $\mathbf{i}_{\mathrm{NL}}$ is the nonlinear distortion, which becomes $\mathbf{d} = \mathbf{T}_{\mathrm{CP}}\mathbf{i}_{\mathrm{NL}}$ after CP insertion. In (34), the nonlinear distortion $\mathbf{d}$, which represents the CCI, is uncorrelated with the linear part $\tilde{\alpha}\mathbf{u}$, which represents the SOI. We assume that the transmitted signal $\mathbf{v}$ passes through a slowly time-varying frequency-selective multipath fading channel, with finite impulse response collected in the vector $\mathbf{h} = [h(0) \cdots h(L-1)\ 0 \cdots 0]^T$), which contains L zero-mean complex Gaussian taps, padded with $K - L$ zeros. At the receiver side, the CP is discarded, and an FFT is performed, thereby obtaining the received vector

$$\mathbf{y} = \widetilde{\alpha}\mathbf{\Lambda}\mathbf{s} + \mathbf{\Lambda}\mathbf{F}\mathbf{i}_{\mathrm{NL}} + \mathbf{n}, \tag{35}$$

where $\mathbf{\Lambda} = \mathrm{Diag}(\boldsymbol{\lambda})$, with $\boldsymbol{\lambda} = [\lambda_0 \ldots \lambda_{K-1}]^T = \mathbf{F}\mathbf{h}$, and $\mathbf{n}$ is the AWGN. By assuming perfect channel-state information, and performing a zero-forcing equalization, we obtain $\mathbf{z} = \widetilde{\alpha}^{-1}\mathbf{\Lambda}^{-1}\mathbf{y} = \mathbf{s} + \widetilde{\alpha}^{-1}\mathbf{F}\mathbf{i}_{\mathrm{NL}} + \widetilde{\alpha}^{-1}\mathbf{\Lambda}^{-1}\mathbf{n}$. By denoting with $[\mathbf{a}]_k$ the kth element of a generic vector $\mathbf{a}$, the decision variable in the kth subcarrier is expressed by $[\mathbf{z}]_k = [\mathbf{s}]_k + \widetilde{\alpha}^{-1}[\mathbf{F}\mathbf{i}_{\mathrm{NL}}]_k + \widetilde{\alpha}^{-1}\lambda_k^{-1}[\mathbf{n}]_k$, or equivalently by

$$r_k[\mathbf{z}]_k = r_k[\mathbf{s}]_k + r_k\widetilde{\alpha}^{-1}[\mathbf{F}\mathbf{i}_{\mathrm{NL}}]_k + e^{-j\arg(\lambda_k)}\widetilde{\alpha}^{-1}[\mathbf{n}]_k, \tag{36}$$

where $r_k = |\lambda_k|$. Clearly, (36) is in the same form of (3), where, in the right-hand side, the first term is the SOI, the second term is the CCI, and the last is the AWGN. Since the number of subcarriers is high, the term $[\mathbf{F}\mathbf{i}_{\mathrm{NL}}]_k$ can be well approximated as Gaussian [12, 13]. Moreover, since the channel taps are zero-mean complex Gaussian, r_k in (36) is a Rayleigh random variable, with the same pdf for all the subcarriers. As a result, by setting $\sigma_{\mathrm{S}}^2 = E\{|[\mathbf{s}]_k|^2\}$, $\sigma_{\mathrm{I}}^2 = |\widetilde{\alpha}|^{-2}E\{|[\mathbf{F}\mathbf{i}_{\mathrm{NL}}]_k|^2\}$, and $\sigma_{\mathrm{N}}^2 = |\widetilde{\alpha}|^{-2}E\{|[\mathbf{n}]_k|^2\}$, the SER for coherent modulations can be expressed by (9). Observe that σ_{S}^2 is independent of the subcarrier index, provided that the same power is used for all the subcarriers k. Similarly, σ_{N}^2 is independent of k because of the white noise assumption. Actually, σ_{I}^2 is slightly dependent from the subcarrier index k, but it is well approximated as constant within the OFDM bandwidth [12]. Therefore, when the same constellation is used for all the subcarriers, the SER is practically independent of the subcarrier index. Note that $|\widetilde{\alpha}|^2$ and $E\{|[\mathbf{F}\mathbf{i}_{\mathrm{NL}}]_k|^2\}$ can be computed using closed form expressions derived from the characteristics of the NLA [12].

Figure 7 shows the SER of an OFDM system with $K = 128$ subcarriers, each one loaded with 16-QAM symbols. In this case, $\alpha = 3$ and $\gamma = 1/5$. A multipath channel with exponential power-delay profile and length $L = 16$ has been used in the simulation. We assume a perfectly predistorted NLA at the transmitter, that is, a clipper of the envelope of the input signal, with an output power back-off (OBO) equal to 3 dB. The SER is plotted versus the receiver SNR, defined as $\rho_{\mathrm{R}} = \Omega(\sigma_{\mathrm{S}}^2+\sigma_{\mathrm{I}}^2)/\sigma_{\mathrm{N}}^2 = \rho_{\mathrm{N}}(\gamma^{-1}+\rho_{\mathrm{I}}^{-1})$, which is the apparent SNR measured at the receiver side. Figure 7 exhibits a good agreement between the theoretical SER and the simulated one. A slight mismatch is present at high SNR. This slight mismatch is not due to our truncation criterion, as verified by its agreement with the lower bound (23). Indeed, despite $K = 128$ is sufficiently high, the CCI, that is, the nonlinear distortion in the frequency domain, is not exactly Gaussian, but only approximately. Anyway, due to the fact that the SER mismatch is really slight, the Gaussian approximation seems to be acceptable.

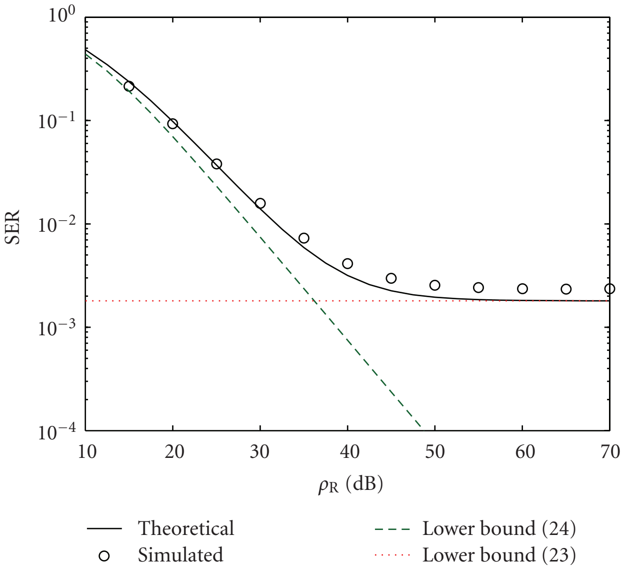

Figure 7: SER in OFDM systems (16-QAM, $K = 128$, $L = 16$, ideal predistortion).

4.2. CDMA with Multiuser Detection and Frequency-Flat Fading. In the downlink of a direct-sequence CDMA system, the vector transmitted in a generic symbol interval can be expressed as $\mathbf{v} = \mathbf{SAb}$ [34], where $\mathbf{b}$ is a column vector of size K containing the independent data symbols of the K active users, $\mathbf{A}$ is the $K \times K$ diagonal matrix containing the signal amplitudes, and $\mathbf{S}$ is the $P \times K$ containing the users' spreading codes, which are assumed real with length P equal to the processing gain. After passing through a slowly time-varying frequency-flat channel with Rayleigh statistic, the vector received by the kth user can be expressed by

$$\mathbf{y}_k = r_k e^{j\theta_k}\mathbf{v} + \boldsymbol{\eta}_k, \tag{37}$$

where $r_k e^{j\theta_k}$ is the channel coefficient experienced by the kth user, and $\boldsymbol{\eta}_k$ is the AWGN vector. Assuming perfect phase estimation $\widehat{\theta}_k = \theta_k$, the received vector after phase compensation can be expressed by $\widetilde{\mathbf{y}}_k = e^{-j\theta_k}\mathbf{y}_k = r_k\mathbf{v} + e^{-j\theta_k}\boldsymbol{\eta}_k = r_k\mathbf{v} + \widetilde{\boldsymbol{\eta}}_k$. In this context, two types of detection methods are considered: a code-matched filter (CMF) detector, which is a simple despreader [34], and an approximated minimum mean-squared error (MMSE) detector, which is a low-complexity version of the linear minimum mean-squared error (LMMSE) multiuser detector [34].

For the CMF detector, the decision vector is obtained by performing the despreading operation

$$\mathbf{z}_{k,\mathrm{CMF}} = \mathbf{S}^H\widetilde{\mathbf{y}}_k = r_k\mathbf{S}^H\mathbf{SAb} + \mathbf{S}^H\widetilde{\boldsymbol{\eta}}_k = r_k\mathbf{RAb} + \mathbf{n}_k, \tag{38}$$

where $\mathbf{z}_{k,\mathrm{CMF}}$ is a column vector of size K that contains, in its kth position, the decision variable of the user k, while $\mathbf{R} = \mathbf{S}^H\mathbf{S}$ contains the crosscorrelation coefficients of the spreading sequences. Therefore, the received symbol of the kth user is expressed by

$$[\mathbf{z}_{k,\mathrm{CMF}}]_k = r_k A_k [\mathbf{b}]_k + r_k \sum_{\substack{j=1\\ j\neq k}}^{K} \rho_{k,j} A_j [\mathbf{b}]_j + [\mathbf{n}_k]_k, \tag{39}$$

where $A_j = [\mathbf{A}]_{j,j}$, $\rho_{k,j} = [\mathbf{R}]_{k,j}$, and $[\mathbf{A}]_{m,n}$ denotes the (m,n)th element of the matrix $\mathbf{A}$. Obviously, (39) is compliant with (3), because the first term is the Rayleigh-faded SOI, the second term represents the CCI, where the fading channel is the same experienced by the SOI, and the last term is the AWGN. Under the assumption that the system attends a high number of users K, for example, $K \geq 20$, and supposing that the K transmitted amplitudes $\{A_j\}_{j=1}^{K}$ are almost equal, such as in satellite downlink channels [11], the CCI term in (39) can be accurately approximated by a Gaussian random variable. By setting $\sigma_{\mathrm{S}}^2 = E\{A_k^2|[\mathbf{b}]_k|^2\}$, $\sigma_{\mathrm{I}}^2 = \sum_{j=1,j\neq k}^{K} \rho_{k,j}^2 A_j^2 E\{|[\mathbf{b}]_j|^2\}$, and $\sigma_{\mathrm{N}}^2 = E\{|[\mathbf{n}_k]_k|^2\}$, the SER for the kth user is expressed by (9).

If we use the LMMSE detector [34], instead of the CMF, the decision vector is obtained as $\mathbf{z}_{k,\mathrm{LMMSE}} = (\mathbf{R} + \sigma_{\eta_k}^2 r_k^{-2}\mathbf{A}^{-2})^{-1}\mathbf{z}_{k,\mathrm{CMF}}$, where $\sigma_{\eta_k}^2$ is the AWGN power, that is, $E\{\boldsymbol{\eta}_k\boldsymbol{\eta}_k^H\} = \sigma_{\eta_k}^2\mathbf{I}_P$. To reduce the computational complexity of the LMMSE receiver, an *approximated minimum mean-squared error (AMMSE)* receiver can be obtained by replacing the instantaneous fading power gain r_k^2 with its average value $\Omega_k = E\{r_k^2\}$ [35]. It is worth noting that the AMMSE detector is the flat-fading counterpart of the precombining LMMSE receiver proposed in [36] for frequency-selective channels. For the AMMSE detector, the decision vector is obtained by left-multiplying the CMF vector $\mathbf{z}_{k,\mathrm{CMF}}$ in (38) with the matrix $\mathbf{X}_k = (\mathbf{R} + \sigma_{\eta_k}^2\Omega_k^{-1}\mathbf{A}^{-2})^{-1}$. Hence, the received symbol of the user k is expressed by

$$\begin{aligned}&[\mathbf{z}_{k,\mathrm{AMMSE}}]_k\\ &\quad = r_k[\mathbf{X}_k\mathbf{RA}]_{k,k}[\mathbf{b}]_k + r_k \sum_{j=1,j\neq k}^{K} [\mathbf{X}_k\mathbf{RA}]_{k,j}[\mathbf{b}]_j + [\mathbf{X}_k\mathbf{n}_k]_k,\end{aligned} \tag{40}$$

which is again in the same form of (3). It is easy to verify that the individual interference terms (one for each interfering user) in (40) have almost equal variance. As a consequence, when the number of active users is sufficiently high, the Gaussian approximation of the CCI is reasonable. Therefore, also in this case the SER for the user k can be expressed by (9), where $\sigma_{\mathrm{S}}^2 = [\mathbf{X}_k\mathbf{RA}]_{k,k}^2 E\{|[\mathbf{b}]_k|^2\}$, $\sigma_{\mathrm{I}}^2 = \sum_{j=1,j\neq k}^{K}[\mathbf{X}_k\mathbf{RA}]_{k,j}^2 E\{|[\mathbf{b}]_j|^2\}$, and $\sigma_{\mathrm{N}}^2 = E\{|[\mathbf{X}_k\mathbf{n}_k]_k|^2\}$. In general, the SER is different from user to user, since the CCI power depends on the crosscorrelation coefficients $\{\rho_{k,j}\}_{k\neq j}$, which in general are not all equal.

Figure 8 highlights the SER performance of the CMF receiver in a downlink CDMA environment with $K = 20$ active users, BPSK modulation (with $\alpha = 1$ and $\gamma = 2$ in (5)), and Gold codes with processing gain $P = 31$. Equal-power users' signals are assumed, that is, $A_k^2 = A^2$. The SER, averaged over all the active users, is plotted versus the user SNR ρ_{U}, defined as $\rho_{\mathrm{U}} = \Omega_k A^2/\sigma_{\eta_k}^2$, which is assumed equal for all the users. In addition, Figure 8 displays that also the SER of the AMMSE detector is accurately modeled by (9).

4.3. *GPS with Transparent Relay.*

GPS is a well known satellite-based system primarily employed for positioning, navigation, and timing purposes [37]. We assume an indoor GPS receiver aided by a fixed outdoor antenna that acts as an outdoor-to-indoor wireless relay [14]. The relay is transparent, that is, nonregenerative. We also assume that the outdoor antenna is placed on the top of the building, in order to maximize the number of visible satellites. This configuration allows for a coarse positioning even when the indoor receiver does not see any satellite.

In GPS, the information bits, BPSK-modulated with rate $f_{\mathrm{b}} = 50$ bps, are transmitted by the satellites using direct-sequence CDMA, with chip rate $f_{\mathrm{c}} = 1.023$ MHz [37]. The spreading sequences, usually referred to as coarse-acquisition (C/A) codes, are Gold codes of length $P = 1023$, which are repeated $N = 20$ times within a bit interval [37]. The signal received by the relay in a generic symbol interval of length NP can be expressed by

$$\mathbf{v} = \sum_{k=1}^{K} b_k A_k \mathbf{D}_k \mathbf{s}_k + \boldsymbol{\eta}_{\mathrm{OUT}}, \tag{41}$$

where K is the number of satellites seen by the relay, b_k is the message bit of the kth satellite, A_k is the amplitude of the kth satellite signal, $\mathbf{D}_k$ is a diagonal matrix that models the Doppler shift f_k due to the satellite motion, expressed by $[\mathbf{D}_k]_m = e^{j(\phi_k + 2\pi m f_k/f_c)}$, where ϕ_k is the initial phase, $\mathbf{s}_k$ is the column vector of size NP that contains the satellite-specific C/A code, and $\boldsymbol{\eta}_{\mathrm{OUT}}$ is the AWGN due to the outdoor receiver. In (41), the multipath effect has been neglected for two reasons. First, since the relay is placed the top of the building, the surrounding objects are few. Second, the multipath effect is usually nonnegligible for those satellites that are near the horizon [37], but their signals can be excluded by conveniently shaping the antenna pattern of the outdoor antenna, since the outdoor antenna sees a sufficient number of satellites with enough elevation. For simplicity of explanation, in (41) we have modeled the K received signals as time-synchronous; we will relax this assumption later on.

After relaying, the GPS signal is received by the indoor detector. Since the L1 frequency ($f_{\mathrm{L1}} = 1.57542$ GHz) is not far from the bands used for third-generation (3G) cellular communications, we can use the indoor channel models developed for 3G systems, where the channel taps are Rayleigh distributed [38]. Multipath effects can be neglected because the maximum delay spread, on the order of few hundreds of nanoseconds [38], is much lower than the chip period $1/f_{\mathrm{c}} \approx 1\,\mu$s. Therefore, the signal received by the indoor receiver can be expressed by $\mathbf{y} = re^{j\theta}\mathbf{v} + \boldsymbol{\eta}_{\mathrm{IN}} = re^{j\theta}\sum_{k=1}^{K} b_k A_k \mathbf{D}_k \mathbf{s}_k + re^{j\theta}\boldsymbol{\eta}_{\mathrm{OUT}} + \boldsymbol{\eta}_{\mathrm{IN}}$, where $re^{j\theta}$ is the channel coefficient, and $\boldsymbol{\eta}_{\mathrm{IN}}$ is the AWGN of the indoor receiver. Assuming perfect compensation for the phase shift and for the Doppler shift of the kth signal, the received signal after despreading can be expressed as $\tilde{y}_k = e^{-j\theta}\mathbf{s}_k^T\mathbf{D}_k^H\mathbf{y}$, which leads to

$$\tilde{y}_k = rb_kA_k + r\sum_{\substack{j=1\\ j\neq k}}^{K} i_{k,j} + rn_{k,\mathrm{OUT}} + n_{k,\mathrm{IN}}, \tag{42}$$

where $i_{k,j} = b_jA_j\mathbf{s}_k^T\mathbf{D}_k^H\mathbf{D}_j\mathbf{s}_j$ is the cross-term contribution due to the non-orthogonality of the Doppler-modified spreading sequences $\mathbf{D}_k\mathbf{s}_k$ and $\mathbf{D}_j\mathbf{s}_j$, $n_{k,\mathrm{OUT}} = \mathbf{s}_k^T\mathbf{D}_k^H\boldsymbol{\eta}_{\mathrm{OUT}}$ is the Gaussian CCI due to the relayed AWGN, and $n_{\mathrm{IN}} = e^{-j\theta}\mathbf{s}_k^T\mathbf{D}_k^H\boldsymbol{\eta}_{\mathrm{IN}}$ is the Gaussian AWGN. Since the maximum Doppler shift is on the order of $f_{\mathrm{MAX}} \approx 5$ kHz, the Doppler-modified spreading sequences $\mathbf{D}_k\mathbf{s}_k$ and $\mathbf{D}_j\mathbf{s}_j$ maintain their low-crosscorrelation properties. Therefore, in (42), the cross-terms $\{i_{k,j}\}$ are usually neglected by conventional receivers [37], with unnoticeable effects especially when $n_{k,\mathrm{OUT}}$ is high. This happens also in the presence of asynchronism among the K received signals [37], since the low-crosscorrelation properties of the Gold codes are maintained for any shift of the spreading sequences. As a result, the BER for the message sent by satellite k can be expressed by (9), with $\sigma_{\mathrm{S}}^2 = A_k^2$, $\sigma_{\mathrm{I}}^2 = E\{|n_{k,\mathrm{OUT}}|^2\}$, $\sigma_{\mathrm{N}}^2 = E\{|n_{k,\mathrm{IN}}|^2\}$, $\alpha = 1$, and $\gamma = 2$.

Figure 9 compares the theoretical BER with the simulated one. We assume that the outdoor antenna sees $K = 6$ satellites, whose signals are asynchronous at the receiver side. Without loss of generality, we focus on the detection of the first satellite signal. The relative delays of the other $K-1$ signals with respect to the first one are randomly generated assuming a uniform distribution between 0 and $P = 1023$ chips. The Doppler shifts $\{f_k\}_{k=1}^K$ are uniformly distributed between $-f_{\mathrm{MAX}}$ and $f_{\mathrm{MAX}} = 5$ kHz. The amplitudes $\{A_k\}_{k=1}^K$ are randomly chosen in order to reflect the different satellite distances from the earth, which are between $d_{\mathrm{MIN}} \approx 20000$ km and $d_{\mathrm{MAX}} \approx 25000$ km [37]. The BER is plotted as a function of the indoor receiver SNR, which coincides with $\rho_{\mathrm{N}}/2$. Figure 9 evidently demonstrates that the proposed analysis well predicts the BER performance for different values of the outdoor antenna SNR, expressed as $\rho_{\mathrm{I}}/2$. In our simulation, the power sum of the cross-terms $\{i_{k,j}\}$ is more than 20 dB lower than the CCI power, thereby validating the correctness of the approximation discussed after (42).

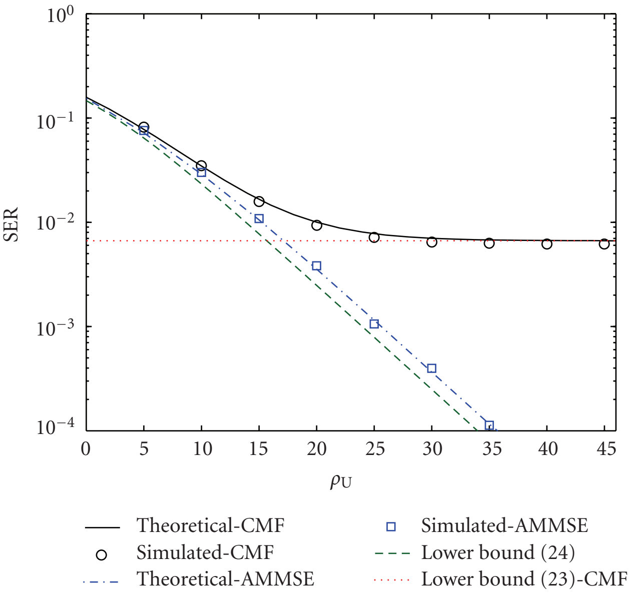

Figure 8: SER in CDMA downlink systems (BPSK, $K = 20$, $P = 31$, Gold codes).

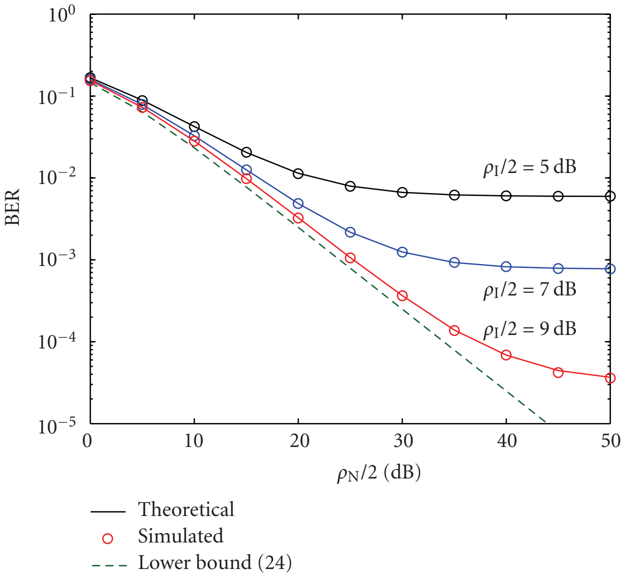

Figure 9: BER in GPS systems with transparent relay ($K = 6$).

5. Concluding Remarks

We have investigated the symbol-error probability of coherent detection schemes in the presence of CCI and Rayleigh fading. We have made two main hypotheses. First, there exists maximal correlation between the fading channels experienced by the SOI and by the CCI. This assumption holds true in many scenarios, for example, when the interference is generated at the transmitter, such as in multiuser downlink systems. Second, the CCI, which is independent of the SOI, can be modeled as Gaussian at the decision variable. This assumption also holds true in many scenarios, such as when the decision variable is obtained by collecting many elements, such as in CDMA or in OFDM systems. We have theoretically calculated the symbol-error probability by using a series expansion of generalized hypergeometric functions. Different features of the proposed approach have been considered, such as an accurate criterion for the series truncation, some alternative closed-form SER expressions, and the effect of phase errors. Moreover, we have shown that the proposed theoretical formula is more accurate than two alternative approaches based on LG quadrature or on MC integration. In addition, we have demonstrated that our analytical findings can be used to foresee the error performances in different scenarios. However, the proposed evaluation method is quite general, and therefore it can be used also in other scenarios, not investigated in this paper, where the SOI and the CCI experience maximally correlated fading channels.

Appendices

A. Analytical Evaluation

By using the substitution $\beta = r/\sqrt{\Omega}$, and setting $\rho_{\mathrm{N}} = \gamma\Omega\sigma_{\mathrm{S}}^2/\sigma_{\mathrm{N}}^2 = \mu^2$ and $\rho_{\mathrm{N}}/\rho_{\mathrm{I}} = \Omega\sigma_{\mathrm{I}}^2/\sigma_{\mathrm{N}}^2 = \lambda^2$, (8) reduces to

$$P_e = 2\alpha \int_0^{+\infty} Q\left(\sqrt{\frac{\beta^2\mu^2}{\beta^2\lambda^2+1}}\right)\beta e^{-\beta^2}\,d\beta. \tag{A.1}$$

Inserting $Q(x) = (1/2)\,\mathrm{erfc}(x/\sqrt{2})$ in (A.1), and using $y = \beta\mu/\sqrt{2+2\beta^2\lambda^2}$, we obtain

$$P_e = 2\alpha\mu^2 \int_0^{\mu/(\sqrt{2}\lambda)} \frac{y}{\left(\mu^2-2\lambda^2y^2\right)^2} e^{-2y^2/(\mu^2-2\lambda^2y^2)}\,\mathrm{erfc}(y)\,dy. \tag{A.2}$$

Integrating (A.2) by parts, and substituting $t = \mu^2 - 2\lambda^2 y^2$, (A.2) becomes

$$P_e = \frac{\alpha}{2} - \frac{\alpha\sqrt{2}}{4\sqrt{\pi}\lambda} e^{(2-\mu^2)/(2\lambda^2)} \int_0^{\mu^2} e^{-\mu^2/(\lambda^2 t)} e^{t/(2\lambda^2)} \left(\mu^2 - t\right)^{-1/2} dt. \tag{A.3}$$

By exploiting the Taylor series expansion of $e^{t/(2\lambda^2)}$, (A.3) can be expressed as

$$\begin{aligned} P_e = {} & \frac{\alpha}{2} - \frac{\alpha\sqrt{2}}{4\sqrt{\pi}\lambda} e^{(2-\mu^2)/(2\lambda^2)} \sum_{k=0}^{+\infty} \frac{1}{k!}\left(\frac{1}{2\lambda^2}\right)^k \\ & \times \int_0^{\mu^2} e^{-\mu^2/(\lambda^2 t)} t^k \left(\mu^2 - t\right)^{-1/2} dt. \end{aligned} \tag{A.4}$$

The integral in (A.4) is in the same form of the integral of Equation 3.471.2 in [17], hence we obtain

$$\begin{aligned} P_e = {} & \frac{\alpha}{2} - \frac{\alpha\sqrt{2}}{4}\frac{\mu}{\lambda} e^{(1-\mu^2)/(2\lambda^2)} \sum_{k=0}^{+\infty} \frac{1}{k!}\left(\frac{\mu^2}{2\lambda^3}\right)^k \\ & \times W_{-(k+1)/2,(k+1)/2}\left(\lambda^{-2}\right), \end{aligned} \tag{A.5}$$

where $W_{a,b}(\cdot)$ is the Whittaker W-function of order a, b [17, 22]. By means of Equation 13.1.33 in [22], (A.5) can also be expressed in terms of the Tricomi U-function, as expressed by

$$P_e = \frac{\alpha}{2} - \frac{\alpha\sqrt{2}}{4}\frac{\mu}{\lambda^3} e^{-\mu^2/(2\lambda^2)} \sum_{k=0}^{+\infty} \frac{1}{k!}\left(\frac{\mu^2}{2\lambda^4}\right)^k U\left(k+\frac{3}{2}, k+2, \lambda^{-2}\right), \tag{A.6}$$

and, using Equation 13.1.10 in [22], in terms of the generalized hypergeometric function ${}_pF_q(\cdot)$ with $p = 2$ and $q = 0$, as expressed by

$$P_e = \frac{\alpha}{2} - \frac{\alpha\sqrt{2}}{4}\mu e^{-\mu^2/(2\lambda^2)} \sum_{k=0}^{+\infty} \frac{1}{k!}\left(\frac{\mu^2}{2\lambda^2}\right)^k {}_2F_0\left(k+\frac{3}{2}, \frac{1}{2};; -\lambda^2\right), \tag{A.7}$$

which is the same of (9).

B. Alternative Expressions

In (9), or equivalently in (A.7), the symbol-error probability is expressed as a series expansion of generalized hypergeometric functions. However, there exist also other symbol-error probability expressions that are equivalent to (A.7). For instance, (A.5) and (A.6) are also expressed as a series expansion of hypergeometric functions, that is, the Whittaker W-function and the Tricomi U-function. In addition, since the generalized hypergeometric function ${}_pF_q(\cdot)$ can be defined by its corresponding series expansion (10), the symbol-error probability (A.7) can be equivalently expressed by a double series as

$$P_e = \frac{\alpha}{2} - \frac{\alpha\sqrt{2}}{4}\mu e^{-\mu^2/(2\lambda^2)} \sum_{k=0}^{+\infty}\sum_{l=0}^{+\infty} \frac{(3/2)_{k+l}(1/2)_l}{(3/2)_k k!\,l!}\left(\frac{\mu^2}{2\lambda^2}\right)^k \left(-\lambda^2\right)^l. \tag{B.1}$$

Besides, the double series (B.1) can be expressed in terms of a unique generalized hypergeometric function, using the Kampé de Fériet's double hypergeometric function $F_{q:s;v}^{p:r;u}[\cdot]$ [39], as expressed by

$$P_e = \frac{\alpha}{2} - \frac{\alpha\sqrt{2}}{4}\mu e^{-\mu^2/(2\lambda^2)} F_{0:1;0}^{1:0;1}\left[\begin{matrix} \frac{3}{2}: & -; & \frac{1}{2}; \\ -: & \frac{3}{2}; & -; \end{matrix}\ \frac{\mu^2}{2\lambda^2}, -\lambda^2\right], \tag{B.2}$$

$$F_{0:1;0}^{1:0;1}\left[\begin{matrix} a: & -; & c; \\ -: & b; & -; \end{matrix}\ x_1, x_2\right] = \sum_{k=0}^{+\infty}\sum_{l=0}^{+\infty} \frac{(a)_{l+k}(c)_l}{(b)_k}\frac{x_1{}^k}{k!}\frac{x_2{}^l}{l!}. \tag{B.3}$$

Acknowledgments

The authors thank Professor M.-S. Alouini for his valuable comments and appreciated suggestions on a previous version of this paper, and Ing. Guido De Angelis for suggesting [14]. They also thank the reviewers for their insightful and constructive comments.

References

[1] M.-S. Alouini and A. Goldsmith, "A unified approach for calculating error rates of linearly modulated signals over generalized fading channels," *IEEE Transactions on Communications*, vol. 47, no. 9, pp. 1324–1334, 1999.

[2] M. K. Simon and M.-S. Alouini, *Digital Communication over Fading Channels*, John Wiley & Sons, New York, NY, USA, 2nd edition, 2005.

[3] R. Krishnamurthi and S. C. Gupta, "Error performance of Gray encoded QPSK and 8-PSK schemes in a fading channel with cochannel interference," *IEEE Transactions on Communications*, vol. 41, no. 12, pp. 1773–1776, 1993.

[4] N. C. Beaulieu and A. A. Abu-Dayya, "Bandwidth efficient QPSK in cochannel interference and fading," *IEEE Transactions on Communications*, vol. 43, no. 9, pp. 2464–2474, 1995.

[5] V. A. Aalo and J. Zhang, "On the effect of cochannel interference on average error rates in Nakagami-fading channels," *IEEE Communications Letters*, vol. 3, no. 5, pp. 136–138, 1999.

[6] M. Chiani, M. Z. Win, A. Zanella, R. K. Mallik, and J. H. Winters, "Bounds and approximations for optimum combining of signals in the presence of multiple cochannel interferers and thermal noise," *IEEE Transactions on Communications*, vol. 51, no. 2, pp. 296–307, 2003.

[7] A. Shah and A. M. Haimovich, "Performance analysis of maximal ratio combining and comparison with optimum combining for mobile radio communications with cochannel interference," *IEEE Transactions on Vehicular Technology*, vol. 49, no. 4, pp. 1454–1463, 2000.

[8] E. Villier, "Performance analysis of optimum combining with multiple interferers in flat Rayleigh fading," *IEEE Transactions on Communications*, vol. 47, no. 10, pp. 1503–1510, 1999.

[9] S. Kundu and S. Chakrabarti, "Outage and BER analysis of cellular CDMA for integrated services with correlated signal and interference," *IEEE Communications Letters*, vol. 7, no. 10, pp. 478–480, 2003.

[10] A. Ligeti, "Outage probability in the presence of correlated lognormal useful and interfering components," *IEEE Communications Letters*, vol. 4, no. 1, pp. 15–17, 2000.

[11] B. R. Vojčić, L. B. Milstein, and R. L. Pickholtz, "Downlink DS CDMA performance over a mobile satellite channel," *IEEE Transactions on Vehicular Technology*, vol. 45, no. 3, pp. 551–560, 1996.

[12] P. Banelli, "Theoretical analysis and performance of OFDM signals in nonlinear fading channels," *IEEE Transactions on Wireless Communications*, vol. 2, no. 2, pp. 284–293, 2003.

[13] D. Dardari, V. Tralli, and A. Vaccari, "A theoretical characterization of nonlinear distortion effects in ofdm systems," *IEEE Transactions on Communications*, vol. 48, no. 10, pp. 1755–1764, 2000.

[14] N. Jardak and N. Samama, "Indoor positioning based on GPS-repeaters: performance enhancement using an open code loop architecture," *IEEE Transactions on Aerospace and Electronic Systems*, vol. 45, no. 1, pp. 347–359, 2009.

[15] P. D. Rahimzadeh and N. C. Beaulieu, "New simple closed-form BER expressions for MRC diversity BPSK in correlated Rayleigh fading and CCI," *IEEE Transactions on Communications*, vol. 57, no. 3, pp. 630–634, 2009.

[16] X. Zhang and N. C. Beaulieu, "A closed-form BER expression for BPSK using MRC in correlated CCI and Rayleigh fading," *IEEE Transactions on Communications*, vol. 55, no. 12, pp. 2249–2252, 2007.

[17] I. S. Gradshteyn and I. M. Ryzhik, *Table of Integrals, Series, and Products*, Academic Press, Amsterdam, The Netherlands, 5th edition, 1994.

[18] F. B. Hildebrand, *Introduction to Numerical Analysis*, Dover, New York, NY, USA, 2nd edition, 1987.

[19] M. J. Juntti and M. Latva-aho, "Bit-error probability analysis of linear receivers for CDMA systems in frequency-selective fading channels," *IEEE Transactions on Communications*, vol. 47, no. 12, pp. 1788–1791, 1999.

[20] L. Rugini and P. Banelli, "BER of OFDM systems impaired by carrier frequency offset in multipath fading channels," *IEEE Transactions on Wireless Communications*, vol. 4, no. 5, pp. 2279–2288, 2005.

[21] A. Annamalai, C. Tellambura, and V. K. Bhargava, "A general method for calculating error probabilities over fading channels," *IEEE Transactions on Communications*, vol. 53, no. 5, pp. 841–852, 2005.

[22] M. Abramowitz and I. A. Stegun, *Handbook of Mathematical Functions: With Formulas, Graphs, and Mathematical Tables*, Dover, New York, NY, USA, 1972.

[23] J. G. Proakis, *Digital Communications*, McGraw-Hill, New York, NY, USA, 4th edition, 2001.

[24] M. Chiani, D. Dardari, and M. K. Simon, "New exponential bounds and approximations for the computation of error probability in fading channels," *IEEE Transactions on Wireless Communications*, vol. 2, no. 4, pp. 840–845, 2003.

[25] Y. Isukapalli and B. D. Rao, "An analytically tractable approximation for the Gaussian Q-function," *IEEE Communications Letters*, vol. 12, no. 9, pp. 669–671, 2008.

[26] K. Cho and D. Yoon, "On the general BER expression of one- and two-dimensional amplitude modulations," *IEEE Transactions on Communications*, vol. 50, no. 7, pp. 1074–1080, 2002.

[27] J. Lu, K. B. Letaief, J. C.-I. Chuang, and M. L. Liou, "M-PSK and M-QAM BER computation using signal-space concepts," *IEEE Transactions on Communications*, vol. 47, no. 2, pp. 181–184, 1999.

[28] P. K. Vitthaladevuni, M.-S. Alouini, and J. C. Kieffer, "Exact BER computation for cross QAM constellations," *IEEE Transactions on Wireless Communications*, vol. 4, no. 6, pp. 3039–3050, 2005.

[29] P. K. Vitthaladevuni and M.-S. Alouini, "A recursive algorithm for the exact BER computation of generalized hierarchical QAM constellations," *IEEE Transactions on Information Theory*, vol. 49, no. 1, pp. 297–307, 2003.

[30] M. K. Simon, *Probability Distributions Involving Gaussian Random Variables*, Springer, New York, NY, USA, 2002.

[31] L. Rugini, P. Banelli, and S. Cacopardi, "Theoretical analysis and performance of the decorrelating detector for DS-CDMA signals in nonlinear channels," *IEEE Transactions on Wireless Communications*, vol. 3, no. 2, pp. 367–372, 2004.

[32] L. Rugini and P. Banelli, "Joint impact of frequency synchronization errors and intermodulation distortion on the performance of multicarrier DS-CDMA systems," *EURASIP Journal on Advances in Signal Processing*, vol. 2005, no. 5, pp. 730–742, 2005.

[33] Z. Wang and G. B. Giannakis, "Wireless multicarrier communications: where Fourier meets Shannon," *IEEE Signal Processing Magazine*, vol. 17, no. 3, pp. 29–48, 2000.

[34] S. Verdú, *Multiuser Detection*, Cambridge University Press, Cambridge, UK, 1998.

[35] L. Rugini, P. Banelli, and S. Cacopardi, "An analytical upper bound on MMSE performance using approximated MMSE multiuser detector in flat Rayleigh fading channels," in *Proceedings of European Wireless*, vol. 2, pp. 952–956, Florence, Italy, February 2002.

[36] M. Latva-aho and M. J. Juntti, "LMMSE detection for DS-CDMA systems in fading channels," *IEEE Transactions on Communications*, vol. 48, no. 2, pp. 194–199, 2000.

[37] E. D. Kaplan and C. Hegarty, *Understanding GPS: Principles and Applications*, Artech House, Boston, Mass, USA, 2nd edition, 2006.

[38] ETSI, "Selection procedures for the choice of radio transmission technologies of the UMTS," Tech. Rep. TR 101 112, April 1998, V3.2.0.

[39] W.-C. C. Chan, K.-Y. Chen, C.-J. Chyan, and H. M. Srivastava, "Some multiple hypergeometric transformations and associated reduction formulas," *Journal of Mathematical Analysis and Applications*, vol. 294, no. 2, pp. 418–437, 2004.